Ultracompact Compton camera for innovative gamma-ray imaging

J. Kataoka [a,*], A. Kishimoto [a], T. Taya [a], S. Mochizuki [a], L. Tagawa [a], A. Koide [a], K. Sueoka [a], H. Morita [a], T. Maruhashi [a], K. Fujieda [a], T. Kurihara [a], M. Arimoto [a], H. Okochi [a], N. Katsumi [a], S. Kinno [a], K. Matsunaga [b], H. Ikeda [b], E. Shimosegawa [b], J. Hatazawa [b], S. Ohsuka [c], T. Toshito [d], M. Kimura [d], Y. Nagao [e], M. Yamaguchi [e], K. Kurita [e], N. Kawachi [e]

[a] Research Institute for Science and Engineering, Waseda University, 3-4-1 Okubo, Shinjuku, Tokyo, 169-8555, Japan
[b] Osaka University Graduate School of Medicine, Medical Imaging Center for Translational Research, Osaka, Japan
[c] Central Research Laboratory, Hamamatsu Photonics K.K., 5000, Hirakuchi, Hamakita-ku, Hamamatsu, Shizuoka, Japan
[d] Nagoya Proton Therapy Center, 1-1-1 Hirate-cho, Kita-ku, Nagoya, Japan
[e] 3National Institutes for Quantum and Radiological Science and Technology, Gunma, Japan

ARTICLE INFO

ABSTRACT

A multipixel photon counter (MPPC) features excellent photon-counting capability as a radiation detector. In particular, a two-plane Compton camera consisting of Ce:GAGG scintillators coupled with MPPC arrays has significant application potential owing to its compact size and low weight. For example, the camera can be easily mounted on a commercial drone to identify radiation hot spots from the sky. In Fukushima, we demonstrated that a ^{137}Cs distribution within a 100 m diameter can be mapped correctly within a couple of tens of minutes. The advanced use of the Compton camera is also anticipated in the field of proton therapy. We evaluated an image of 511 keV annihilation gamma-rays emitted from a PMMA phantom irradiated by 200 MeV protons to mimic an in-beam monitor for proton therapy. Finally, we developed an ultracompact Compton camera (weight = 580 g), for 3-D multicolor molecular imaging. In order to demonstrate the performance capabilities of the device, ^{131}I (365 keV) ,^{85}SrCl$_2$ (514 keV), and ^{65}ZnCl$_2$ (1116 keV) were injected into a living mouse and the data were taken from 12 angles with a total acquisition time of 2 h. We confirmed that all tracers had accumulated on the target organs of the thyroid, bone, and liver, and that the obtained 3-D image was quantitatively correct with an accuracy of ±20%.

1. Introduction

The gamma-ray imaging of sub-MeV to several MeV photons is generally difficult owing to the dominance of Compton scattering over photo-absorption, and is lagging behind the X-ray imaging techniques such as computer tomography (X-ray CT). However, most gamma-ray lines emitted from nuclear reactions are clustered in this range, opening up various opportunities for future applications. For example, single photon emission computer tomography (SPECT) and positron emission tomography (PET) scans are the two most common techniques used in molecular imaging; however, available radioactive tracers are limited either by their energy range or by the difficulties in production and delivery. Thus the gamma-ray imaging of arbitrary energies in the sub-MeV to several MeV region may lead to the discovery of new tracers, which are not yet utilized in the current modalities.

In the field of astronomy, deep gamma-ray observations of MeV sky is also anticipated because detections of gamma-ray lines would provide a direct indication of nucleosynthesis in the universe. In fact, COMPTEL onboard Compton gamma-ray observatory [1] successfully mapped 1.8 MeV gamma-rays emitted from ^{26}Al along the Galactic plane [2]; although there has been no substantial progress in MeV astronomy in the 20 years since. New technologies for sub-MeV to MeV gamma-ray imaging would provide a breakthrough in the field of physics and astronomy [3].

A Compton camera utilizes the kinematics of Compton scattering for imaging, and therefore offers various advantages for detector design [4,5]. In particular, this type of camera does not require heavy mechanical collimators and/or a coded mask, and it features a wide field-of-view and high detection efficiency. Since 2013, we have been
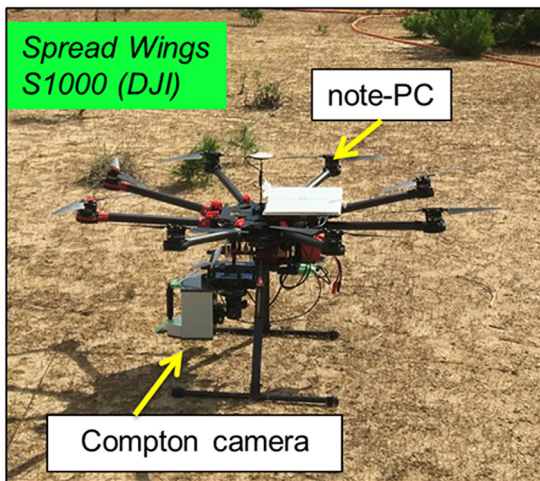
Fig. 1. Photo of the drone (DJI S1000 +) with the Compton camera attached, prior to the flight.

developing a two-plane Compton camera consisting of Ce:GAGG scintillator arrays coupled with large-area multipixel photoncounter (MPPC) arrays [6]. Owing to the thin and compact features of MPPC device, we were able to restrict the dimension of the first product to a very small size and to a low weight (1.9 kg), whilst at the same time achieving excellent sensitivity [7,8]. This paper presents the current status and most recent progress of MPPC-based Compton camera for environment and medical applications.

2. Gamma-ray snapshots using a drone in Fukushima

Considerable amounts of radioactive substances (mainly ^{137}Cs and ^{134}Cs) were released into the environment after the Japanese nuclear disaster in 2011. Owing to the successive and effective decontamination operations to date, some areas had their restrictions lifted in April 2017. However, the distribution of radioactive substances in vast areas of mountains and forests are still unknown, even though such areas occupy more than 70% of Fukushima prefecture. An aerial survey is an effective way to find local hot spots in a region of interest quickly. However, unmanned helicopters are not commonly used due to the high cost (~1M USD) and large size (3.63 m long; 94 kg weight) required to carry bulky detector systems, and therefore previous research is limited [9]. We therefore propose an alternative aerial system using a commercial drone, DJI S1000 + [10], which is relatively cheap (~6K USD) and compact (~1.0 m diagonal wheelbase; 4.2 kg weight) [10]. An obvious disadvantage of using such a drone is that the maximum payload and flight time are both limited to ~5 kg and 15 min, respectively. Therefore, only a low-weight, high sensitivity Compton camera may be suitable for the system.

As the first attempt of aerial gamma-ray imaging, we mounted a compact Compton camera (1.9 kg weight as described above; [6]) onboard a drone to take snapshots of a schoolyard in Namie city, Fukushima. We developed a dedicated wireless communication system between the drone and ground station for real-time imaging. Fig. 1 shows a photo of the detector system being readied for a flight. Fig. 2(a) shows a reference map of the dose rate covering the entire schoolyard (100 m × 80 m) that was generated by using a survey meter prior to the flight. The air dose rate map at an arbitrary point in the schoolyard was approximated by interpolating the data of 30 sampling points spaced every 20×20 m steps. Although the measurement points may be too few to determine the correct dose distribution, the high-dose region (typically 10 µSv/h) clearly traces the distribution of the pine trees near the edge of the schoolyard, while the low dose is near the center (~5 µSv/h).
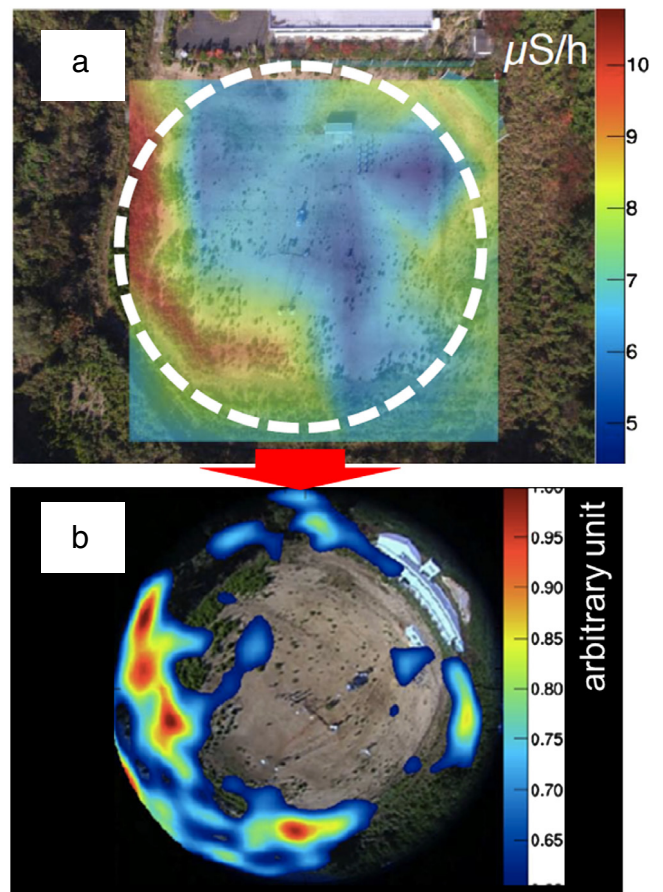

Fig. 2. *Top*: radiation dose map of a schoolyard in Namie, Fukushima, reconstructed from multiple ground-based measurements. A dashed white circle indicates the approximate field-of-view of a Compton camera onboard a drone from 20-m above. *Bottom*: gamma-ray snapshots from 20-m above using a drone.

Fig. 2(b) shows an example aerial snapshot from 20 m above, in which the results were combined for the two flights to increase the photon statistics, with a net measurement time of 25 min. A dashed white circle in Fig. 2(a) indicates the field of the Compton camera from 20 m above. The angular resolution of the Compton camera was $\Delta\theta \simeq 14°$ (FWHM) at 662 keV, and therefore the spatial resolution ranged from 4 m to 10 m, depending on the location in the field-of-view. Although the map is presented in a fisheye view, and is therefore not directly compatible with Fig. 2(a), the gamma-ray image converged to the pine bush on the left as expected. Given that the ground based measurements took more than 3 h and even with the sparse sampling of Fig. 2(a), the aerial snapshot using a drone has the advantage of reducing the measurement time, and will provide more accurate positions of the radiation hot spots.

3. Prompt gamma-ray imaging for proton therapy

Proton therapy is an advanced cancer therapy that uses a feature known as the Bragg peak. Owing to its high concentration of radiation dose, the proton beam can effectively damage tumors, but high precision is required both in treatment planning and the monitoring of dose delivery. The most common method of proton range verification is an offline imaging of annihilation (511 keV) gamma-rays using PET scanners, as PET gantry cannot coexists with a clinical beam. Although various attempts have been made toward in-beam PET imaging [11,12], the distribution of β^+ nuclei which emit 511 keV gamma-rays, is not directly comparable to the proton dose distribution. Instead, it has been
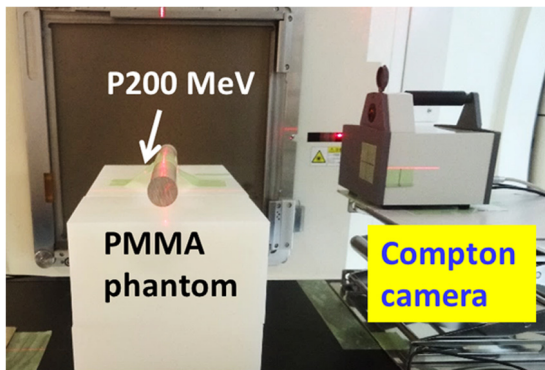
2

Fig. 3. Photo of experimental setup for prompt gamma-ray imaging during 200 MeV proton irradiation at Nagoya Proton Therapy Center.
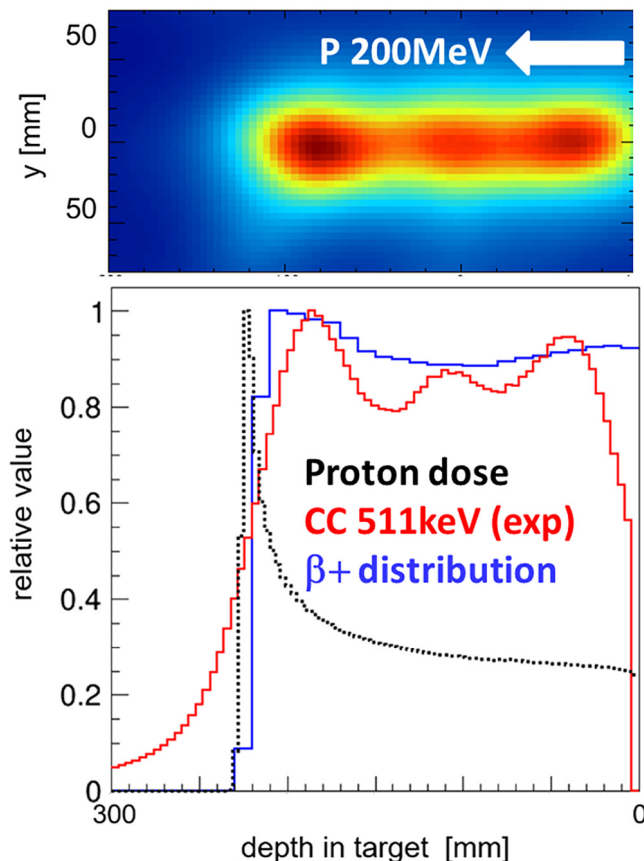

Fig. 4. Prompt gamma-ray imaging of 511 keV using a handheld Compton camera. A PMMA phantom was irradiated by a 200 MeV proton pencil beam.

Fig. 5. Reconstructed 2-D and 3-D color gamma-ray images of a mouse confirming the different concentrations of ^{131}I (364 keV), ^{85}Sr (514 keV) and ^{65}Zn (1116 keV), shown in green, blue, and red, respectively. (For interpretation of the references to color in this figure legend, the reader is referred to the web version of this article.)

argued that some prompt gamma-rays, such as 4.4 MeV photons emitted from ^{12}C and ^{16}O, trace the delivered radiation dose of protons owing to minimum energy threshold of nuclear reactions [13]. Therefore, the possibility of in-beam imaging of prompt gamma-rays with a Compton camera is probable [14].

As a first trial of in-beam imaging using a Compton camera, we evaluated the image of 511 keV gamma-rays emitted from a PMMA phantom while being irradiated by 200 MeV protons, with an update product of a handheld Compton camera [7]. The schematic view of the experiment is shown in Fig. 3. The revised camera offers improved sensitivity and an angular resolution of $\Delta\theta \simeq 8°$(FWHM) at 662 keV, by incorporating 3-D position sensitive scintillators [15]. As shown in Fig. 4, the reconstructed images effectively traced the simulated 1-D
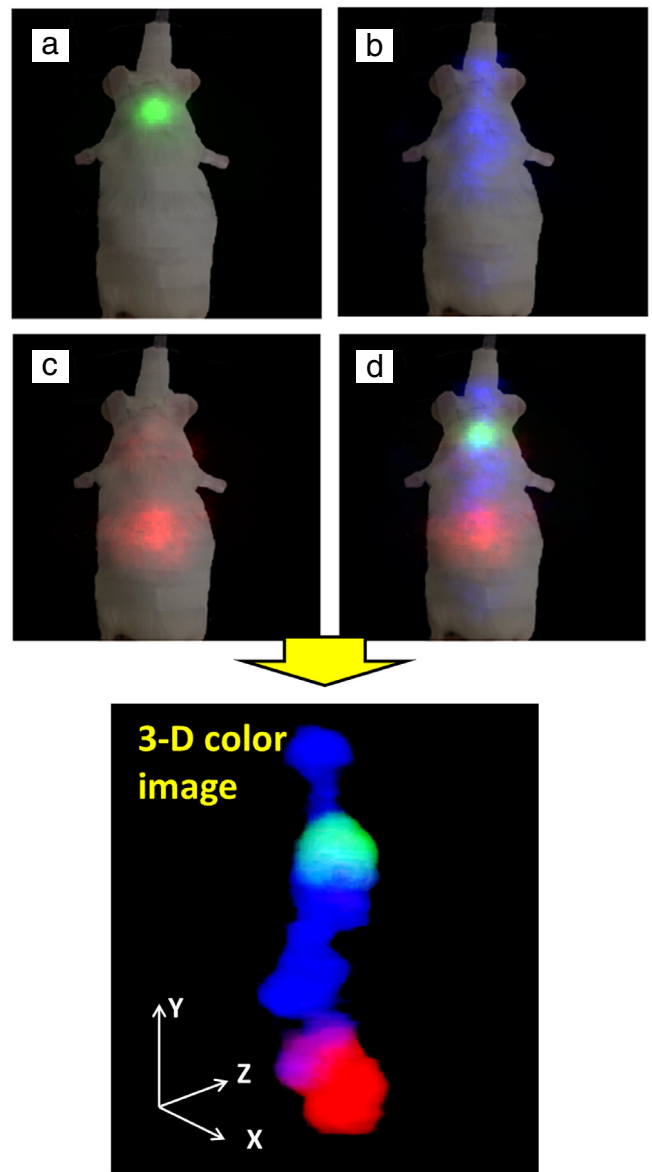
distribution of β^+ nuclei that emit 511 keV gamma-rays. In the next step, we fabricated a Compton camera that features precise imaging of high energy prompt gamma-rays, in particular 4.4 MeV photons. The first preliminary results of the imaging test are presented in a companion paper in this volume [16].

4. 3-D multicolor *in vivo* imaging of a mouse

The SPECT and PET are highly valuable and widely used for diagnosis at the early stage of diseases such as cancer and Alzheimer's. However, owing to the use of a collimator to restrict the direction of the incident gamma-rays, SPECT are generally used only below 300 keV. PET can provide higher resolution image but only applicable to 511 keV annihilation gamma-rays. Moreover, PET tracers such as 18F-FDG (FDG: Fluoro-deoxy-glucose) are usually produced by the cyclotron facility in each medical center, that inevitably increase the cost for diagnosis. In this context, the use of Compton camera to utilize a wider
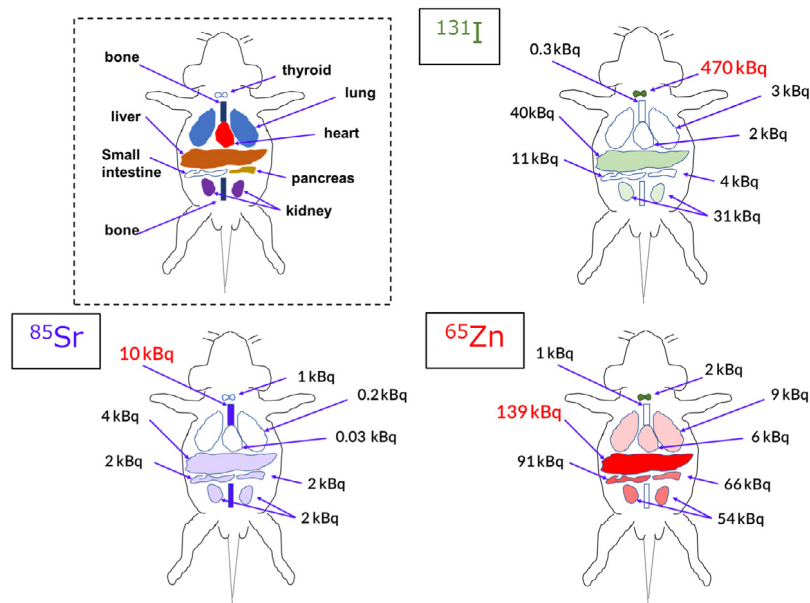
Fig. 6. Accurate experimental RI intensities as measured with an H–Ge detector. The radioactive intensity was sharply concentrated on the thyroid as measured by the 364 keV peak from ^{131}I. In contrast, ^{85}Sr and ^{65}Zn are widely distributed. Particularly, substantial uptake of ^{65}Zn not only in the liver but also in the lung, heart, intestine, spleen and pancreas were clearly seen.

range of radionuclides that were never available before, is eagerly awaited. Moreover, it may enable the simultaneous imaging of multiple tracers [17–19].

In 2016, we successfully developed an ultracompact Compton camera with a weight of only 580 g and an excellent angular resolution of $\Delta\theta \simeq 4.2°$(FWHM) as measured at 662 keV [20]. This corresponds to a spatial resolution of $\simeq$3 mm for a small animal imaging, assuming a subject distance of 40 mm. Moreover, we developed a novel 3-D image reconstruction method and carefully investigated the accuracy of the reconstructed image using a diffuse source with planar geometry. After multiple pre-clinical evaluation we succeeded, for the first time, 3-D imaging of a living mouse within 2 h [21].

Fig. 5 shows tri-color fusion images of 365 keV (^{131}I: *green*), 514 keV (^{85}Sr: *blue*), and 1116 keV (^{65}Zn: *red*) gamma-rays reconstructed using data accumulated from 12-angle around the mouse. For the quantitative performance evaluation, the thyroid, liver, and other organs were harvested 8 h after the experiment and the accurate experimental RI intensities were measured using an HPGe detector. The results are schematically shown in Fig. 6. Note that the radioactive intensity is sharply concentrated on the thyroid as measured by 364 keV peak from ^{131}I. In contrast, the distributions of ^{85}Sr and ^{65}Zn are widely distributed, as indicated in each of gamma-ray images of Fig. 5. Moreover, substantial uptake of ^{65}Zn were not only observed in the liver, but also in the lung, heart, intestine, spleen and pancreas. We therefore confirmed that the relative intensity of the reconstructed image is correct within an accuracy of $\pm$20% [9].

5. Discussion and future prospects

This paper presented recent progress of a two-plane Compton camera based on scintillators coupled with the MPPC for applications in environmental and medical imaging. Compared to other Compton cameras based on semiconductor devices, such as Ge strips and Si–CdTe detectors (e.g., [17–19]), our Compton camera has both strengths and weaknesses depending on the application purposes. The obvious advantages are that (1) the camera can be very compact and light weight, as it does not need any cooling or cryogenic systems, (2) a high sensitivity can be achieved owing to a thick, and heavy (i.e., high-Z) scintillator array, and (3) it has a fast time response and simple data acquisition system owing to internal multiplication of MPPC device.

In contrast, the spatial and/or spectral energy resolutions are not superior to semiconductor devices, even though substantial improvement has been achieved for the medical Compton camera as presented in Section 4. The achieved $\simeq$3 mm spatial resolution appears to be the best for a scintillator-based Compton camera, but further improvements are necessary for small animal imaging. We are therefore fabricating a high-resolution Compton camera based on new scintillator arrays that will be reported elsewhere.

Another shortcomings is that the Compton camera presented in this paper is applicable only for $\geq$ 250 keV photons, due to dominance of photoabsorption over the Compton scattering in the scatterer. The situation is the same for Ge-based Compton camera as described above. In contrast, Si–CdTe-based Compton camera can work even below 100 keV because low-Z material (Si) is used for a scatterer. Since low-energy applications of Compton camera are also beneficial in replacing SPECT imaging (e.g., ^{99m}Tc at around 140 keV), we are testing a fine-pixel plastic scintillator array as a scatterer, however efficiencies in the high energy gamma-ray imaging will be substantially reduced. In general, the features of high sensitivity, a wide energy range, and good angular/energy resolution are opposite to that of the demand, therefore users should have the flexibility when choosing optimum detectors for their own purposes.

References

[1] V. Schonfelder, et al., Astroph. J. Suppl. Series 86 (1993) 657.
[2] R. Diehl, et al., Astron. Astrophys. 298 (1995) 445.
[3] J. Knödlseder, C. R. Physique 17 (2016) 663.
[4] V. Schonfelder, et al., Nucl. Instrum. Methods 107 (1973) 385.
[5] R.W. Todd, J.M. Nightingale, D.B. Evertt, Nature 251 (1974) 132.
[6] J. Kataoka, et al., Nucl. Instrum. Methods A 732 (2013) 403.
[7] A. Kishimoto, et al., J. Instrum. 9 (2014) P11025 8.
[8] J. Kataoka, et al., Nucl. Instrum. Methods A. 784 (2013) 248.
[9] Y. Shikaze, et al., J. Nucl. Sci. Technol. 53 (2016) 1907.
[10] S. Mochizuki, submitted for publication.
[11] T. Nishio, et al., Int. J. Radiat. Oncol. 76 (2010) 277.
[12] H. Tashima, et al., Phys. Med. Biol. 61 (2016) 1795.

[13] M. Moteabbed, S. Espana, H. Paganetti, Phys. Med. Biol. 56 (2011) 1063.

[14] T. Taya, et al., J. Instrum. 12 (2017) P07015.

[15] A. Kishimoto, et al., IEEE Trans. Nucl. Sci. 60 (2013) 3.

[16] A. Koide, in this volume.

[17] S. Motomura, et al., IEEE Trans. Nucl. Sci. 54 (2007) 710.

[18] S. Motomura, et al., J. Anal. At. Spectrom 28 (2013) 934.

[19] S. Takeda, et al., IEEE Trans. Nucl. Sci. 59 (2012) 70.

[20] A. Kishimoto, et al., Nucl. Instrum. Methods A. 845 (2017) 656.

[21] A. Kishimoto, et al., Sci. Rep. 7 (2017) 2110.